Jurnal Kejuruteraan 37(3) 2025: 1099-1116
https://doi.org/10.17576/jkukm-2025-37(3)-03

Strength Performance of Two-Hollow Interlocking Concrete Block Inclusion with Recycled Concrete Aggregate as A Replacement of Natural Fine Aggregate

Nur Syahirah Binti Othman, Noorsuhada Md Nor*, Soffian Noor Mat Saliah & Masyitah Md Nujid

Faculty of Civil Engineering, Universiti Teknologi MARA, Cawangan Pulau Pinang, Permatang Pauh Campus, Pulau Pinang, Malaysia

**Corresponding author: ida_nsn@uitm.edu.my*

Received 14 August 2024, Received inrevised form 26 December 2024
Accepted 26 June 2025, Available online 30 May 2025

ABSTRACT

One of the major challenges facing the construction industry today is the effective management of demolition waste, particularly concrete debris from old structures. Recycling this concrete as aggregate offers a sustainable alternative that reduces dependence on natural resources such as sand, thereby mitigating environmental degradation. This study aims to evaluate the bending (flexural) strength of Two-Hollow Interlocking Concrete Blocks (THICB) incorporating 50% recycled concrete aggregate under three-point loading conditions. A 1:4 concrete mix was prepared using cement, 50% natural sand, 50% RCA, 1% Sika ViscoCrete-2192, and water. Three types of specimens were produced: cubes, Solid Interlocking Concrete Blocks (SICB), and THICBs. A series of tests were conducted, including compressive strength, flexural strength, water absorption, and workability (flow table). Flexural strength performance of THICBs (360 mm × 100 mm × 100 mm) was compared to SICBs after 7, 14, and 28 days of water curing. The compressive strength of RCA mortar cubes reached a maximum of 34.69 MPa at 28 days, indicating good material maturity. Although SICBs recorded a slightly higher ultimate load (14.46 kN), THICBs achieved a notable flexural capacity of 14.06 kN, attributed to their geometric configuration which enhances flexibility under bending. The findings confirm that RCA can be effectively utilized in producing interlocking concrete blocks with satisfactory mechanical performance and compliance with water absorption standards for structural applications. The integration of recycled materials not only supports environmental conservation but also promotes the development of sustainable, durable, and cost-effective building components. This research underscores the potential for commercializing RCA-based interlocking blocks as a viable and eco-friendly solution for future construction practices.

Keywords: recycled concrete aggregates; interlocking concrete bloc; two-hollow interlocking concrete blocks; flexural strength.

INTRODUCTION

There is a rising trend (Maysam et al. 2022) to incorporate sustainable approaches in concrete production using waste materials, including recycled concrete aggregate (RCA). Limited natural fine aggregate supplies (Chung et al. 2023) and difficulties with replacements call for thorough scrutiny of drawbacks (Ruslan et al. 2024), typically offset by adding supplements for durability and robustness. Research shows comparable strengths achieved by alternative material composites (Awoyera et al. 2021; Vázquez et al. 2016). The construction industry faces growing pressure to integrate sustainability concepts, especially since swifter urban development yields vast quantities of construction and demolition waste (C&DW). The global per capita demand for aggregates reaches 3.8 tonnes (Chandru et al. 2023). Limited processing facilities, industry ignorance, and scarce research hold back RCA use in ICBs (Nawaz et al. 2022; Bao, 2023; Zhang et al. 2023; Abera, 2022). Resource consumption and scarcity of natural resources like

sand have become pressing issues as demand increases in developed and developing nations. Furthermore, the effective, sustainable management of CDW is another challenge (Sanjay et al. 2022). Mortarless masonry advances facilitate higher productivity, efficiency, and reduced reliance on skilled labor (Al-Fakih et al. 2022; Mohamed et al. 2024). Utilizing RCA in interlocking concrete blocks (ICBs) has become popular ((Uygunog˘lu et al. 2012) due to population growth and the need for affordable yet eco-friendly alternatives (Correia Lopes et al. 2018; Klemun et al. 2022). Greater research collaboration and industry involvement can overcome obstacles and promote more accountable, sustainable construction techniques (Ruslan et al. 2024).

Concrete is becoming the most used building material for almost any kind of construction project (Hani et al. 2024; Abro et al. 2022). Managing waste from the demolition of aging structures is a significant issue in the building industry. Reusing old concrete helps to conserve natural resources like gravel and sand, which in turn reduces the rate of resource depletion and the amount of landfill space needed. Extensive research has focused on the properties of RCA, which consists of both natural aggregate and leftovers of hardened cement paste attached to it. According to Rifa et al. (2023), there's a gap in research comparing RCA to other alternative materials as fine aggregates. The composition of RCA, determined by the makeup of the original concrete, affects its properties. RCA usually has higher porosity than natural aggregate, affecting its water absorption and specific density (Le et al. 2020). The comparable value of compressive strength for the demolished reinforced concrete structure and precast column was C40/50, while the strength class of the original concrete cubes was C30/37 (Radonjanin et al. 2013). Nevertheless, there are potential benefits to its use.

The construction industry continuously seeks out new ways to boost efficiency and optimize the use of available materials. For instance, improvements in the manufacture of ICBs are being pursued to enhance their performance (Nor et al. 2023). ICBs are precast units that fit together without requiring mortar, forming strong, puzzle-like connections. They provide an efficient building method, but traditionally rely on natural resources. This study explores the possibility of increasing the sustainability of ICBs by incorporating RCA as a substitute for natural fine aggregates. By doing so, we can address the scarcity of natural sand and manage construction waste effectively while maintaining or even improving the strength and durability of ICBs (Patra et al. 2022). The goal is to demonstrate that RCA can serve as a viable and environmentally friendly component in the production of ICBs, ultimately contributing to a more sustainable construction industry.

However, comprehensive experimental testing and data analysis are essential for evaluating structural performance, especially considering the varied strengths associated with different designs of interlocking concrete blocks. Experimental testing was conducted to examine the structural characteristics of ICB incorporating RCA as a partial replacement for sand. Flexural strength was measured using a three-point bending setup, where the sample was supported at both ends, and the load was applied at the midpoint. The maximum stress experienced by the tension side of the sample at the point of failure represents the ultimate flexural strength of the material. An extensive evaluation of the overall efficiency of RCA has been conducted, encompassing assessments of both fresh and hardened concrete properties. Key aspects considered in the review include the ease of working with RCA, the air entrainment within the concrete mix, and the various measures of strength such as compressive, and flexural resistance, as well as density (Kim, 2022; Şimşek et al. 2022).

METHODOLOGY

The methodology summary for this research study is illustrated in Figure 1. The study started with the materials preparation that insist with 4 elements. All materials employed in the research were carefully prepared according to a mixed design ratio of 1:4. The mixture comprises type I Ordinary Portland Cement (OPC), a partial replacement of RCA as fine aggregate, a partial use of natural fine aggregate (sand), water, and superplasticizer (specifically Sika ViscoCrete-2192). The process of producing RCA entailed breaking concrete cubes, crushing them into smaller pieces, and then sieving to obtain the desired aggregate size.

Three types of samples were then created for experimentation: cubes, two-hollow interlocking concrete blocks (THICB), and solid interlocking concrete blocks (SICB). Various tests were conducted in the experiments, including flexural, compression, water absorption, and flow table tests, yielding results such as flexural strength, compressive strength, and concrete properties.

The study focus lies on employing mortar as the primary mixture, with its composition varying based on desired characteristics and specific project requirements. In this instance, the mixture comprises a ratio of 1 part cement to 4 parts aggregates, where aggregates consist of 2 parts natural fine aggregate (sand) and 2 parts fine aggregate replacement, namely RCA. OPC and fine aggregates are mixed with water in each batch, maintaining a water-cement ratio of 0.65, while the RCA partially substitutes the fine aggregate according to a predetermined percentage for the sample. Additionally, a superplasticizer admixture is

incorporated into the mortar mix. The superplasticizer was added to the concrete mixture in order to strengthen the mortar, reduce shrinkage and cracking, and improve the concrete's flowability without the need for more water (Li et al. 2023). The adhesive was OPC, but the superplasticizer enhanced the strength and workability. Detailed preparation of materials is shown in Table 1

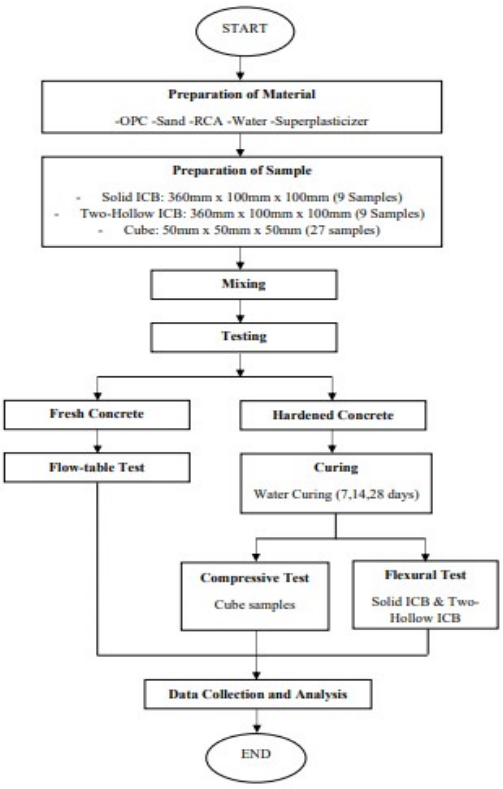

FIGURE 1. The process flow of the study

.

Compression analysis, a technique utilized to ascertain concrete strength and performance under compression, is conducted. Twenty-seven concrete cube samples measuring 50 mm x 50 mm x 50 mm undergo compression testing using a compression machine, aiming to establish parameters such as strain, stress, and deformation. The evaluation occurs at different intervals – 7, 14, and, 28 days post-mould removal and curing process completion. Then the concrete cube was placed on the steel plate and compressed until failure. It was repeated three times to obtain average results for each interval.

The flexural strength examination involved two types of concrete blocks: THICB sized at 360 mm x 100 mm x 100 mm and SICB. These blocks were cured in water for durations of 7, 14, and 28 days. The testing procedure adhered to the specifications outlined in BS EN 13523-7:2001 and was conducted using a 100 kN universal testing machine (UTM). Load application was centered on each concrete block, with the span between the supports set at 270 mm. The mortar is the primary mixture analyzed, the composition of which depends on the desired properties and the specific project requirements (Chen et al. 2022).

PREPARATION OF RECYCLED CONCRETE AGGREGATES

The process of replacing fine aggregates with RCA was conducted in four distinct stages, as illustrated in Figure 2. This method is similar to the procedures reported by Chandru et al. (2023) and Tam et al. (2017). Figure 3 presents the particle size distribution of natural sand and RCA, both of which exhibit comparable grading trends in terms of percentage distribution.

In the first stage, concrete waste was collected from construction sites and laboratory sources. This included test samples, surplus material from construction activities, and debris from demolished structures. In the second stage, the collected concrete was manually broken into smaller pieces using a sledgehammer and a hand drill, facilitating easier handling during subsequent processing.

The third stage involved further reduction of the material size using a jaw crusher, producing particles typically within the 5–10 mm range. In the final stage, the crushed material underwent a complete recycling process—including crushing, washing, and screening—at a designated waste recycling facility. The RCA was then sorted into three size fractions: 0–5 mm, 5–10 mm, and >10 mm (Zhu et al., 2015). For this study, the 0–5 mm fraction was selected as a replacement for natural fine aggregates.

TABLE 1. Detailed preparation of samples

Sample	RCA (kg)	Sand (kg)	Cement (kg)	Water (kg)	Superplasticizer (kg)
Cube	3.378	3.486	1.587	1.032	0.016
SICB	16.623	36.504	35.381	10.805	0.166
THICB	16.623	36.504	35.381	10.805	0.166
Total (kg)	36.624	76.494	72.349	22.642	0.348

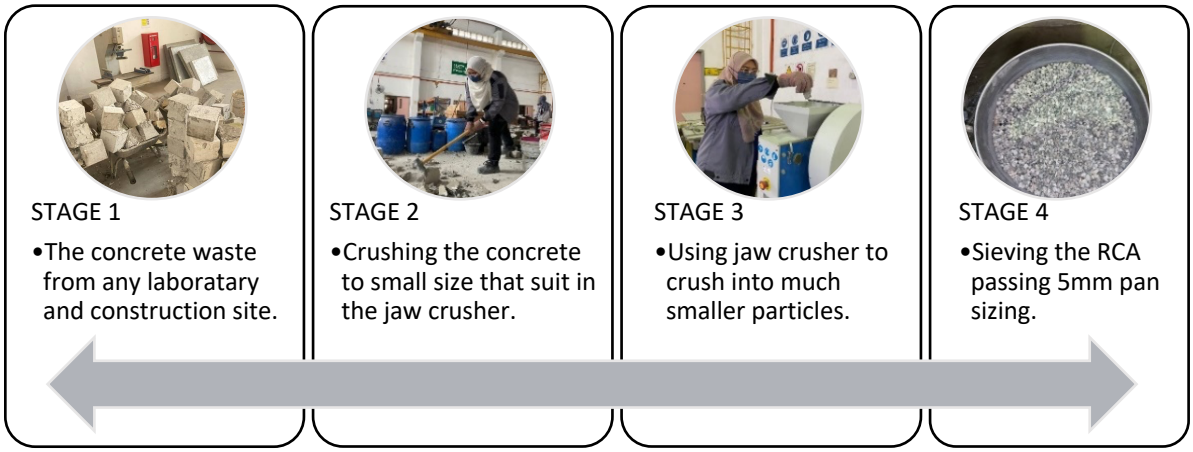

FIGURE 2. The process of the recycled concrete aggregates

In the last step of the procedure, the crushed concrete was screened with a 5 mm screening machine to make sure that only aggregates that were no larger than 5 mm were kept. The crushed concrete was sieved by this machine so that only particles no larger than 5 mm could pass through. The elimination of any larger particles produced RCA with a constant maximum size. This made the recycled concrete aggregate's qualities consistent and homogenous. The fine particles in the concrete mixture were continuously replaced by the aggregate produced by this method.

PARTICLE SIZE DISTRIBUTION AGGREGATES

The maximum weight of 0.3137 kg was found for RCA on the 0.425 µm sieve, according to the results shown in Table 2. Likewise, 0.2889 kg was the maximum weight of sand on the same filter size. Subsequent investigation reveals that 91.57% of RCA candidates passed the aggregate exam. The remainder of the percentage is equivalent to an 8.43% mass retention. A percentage of 98.33% and a mass retention of 1.67% were obtained when the fine aggregate was replaced.

This indicates the percentage of sand passing through the sieve. RCA accounted for 93.71% of the aggregate passing through, while 6.29% of the mass was retained. In particular, 1.25% of the mass was retained to replace the fine aggregate, and 98.75% of the aggregate passed. According to the IS 383-1970 Sieve Standard, both the RCA and natural fine aggregates were within the limits of the Zone II fineness modulus and ranged from 2.1 to 3.37 mm. Additionally, the role of fine aggregates was fulfilled by utilizing natural river sand, which had been processed to pass through a #4 sieve (4.75mm) (Shaikh et al. 2022). This ensured a uniform gradation suitable for the intended application within the concrete mixture.

These small adjustments produced positive outcomes since RCA's mechanical characteristics made it a good replacement for fine aggregates in mortar mixtures (Al-Fakih et al. 2018). The particle size distributions of RCA in Figure 4(a) and sand in Figure 4(b) are contrasted in Figure 4. It is evident that 70.25% of sand and 70.44% of RCA particles, which have a size of 1.7 mm, that pass through the sieve with the similar particle percentage distribution of sand and RCA. Infer from the ASTM C144-11 curve that the types of RCA and fine aggregate of sand employed in this experiment fell within well-graded categories because the curve grew linearly between particle sizes of 0.075 mm and 5 mm. Also, the curve shape was not having a huge gap. In other words, the data was curve smoothly for both of them and have a similar distribution.

PREPARATION OF THE INTERLOCKING BLOCK SAMPLES

A single sheet of plywood was utilized to construct the formwork necessary for casting the interlocking concrete blocks for the study. This custom-made mould was specifically designed to accommodate three individual specimens. A PVC pipe was inserted into this arrangement to support and stabilise the hollow spaces that were meant to mould the specimens. The formwork seemed visually dependable and was an acceptable condition, as shown in Figure 5(a). Although screws were used to link different parts of the formwork, screw connections were chosen because they were simple to remove with a screwdriver and allowed for the manufacture of more than three interlocking concrete block productions. RCA replaced 50% of the conventional sand (Nor et al. 2023) component in the concrete mixture used in the study, which had a ratio of 1:4. For comparison, a control combination without superplasticizer or RCA was also used. Before testing, the samples were thereafter allowed to cure for 7, 14, and 28 days.

TABLE 2. The particle aggregate size distribution of sand and RCA

Sieve Pan (mm)	Sand			RCA		
	Accumulative Retain (kg)	% Mass Retain	% Passing	Accumulative Retain (kg)	% Mass Retain	% Passing
5.00	0.0000	0.00	100.00	0.0000	0.00	100.00
4.75	0.0629	6.29	93.71	0.0843	8.43	91.57
3.35	0.1127	11.27	88.73	0.2047	20.47	79.53
2.00	0.2125	21.25	78.75	0.2644	26.44	73.56
1.70	0.2956	29.56	70.44	0.2975	29.75	70.25
0.425	0.5845	58.45	41.55	0.6112	61.12	38.88
0.300	0.6384	63.84	36.16	0.6917	69.17	30.83
0.212	0.8073	80.73	19.27	0.8736	87.36	12.64
0.150	0.8969	89.69	10.31	0.9588	95.88	4.12
0.075	0.9774	97.74	2.26	0.9862	98.62	1.38
Bottom Pan	1.0000	100.00	0.00	1.0000	100.00	0.00

Ultimate size

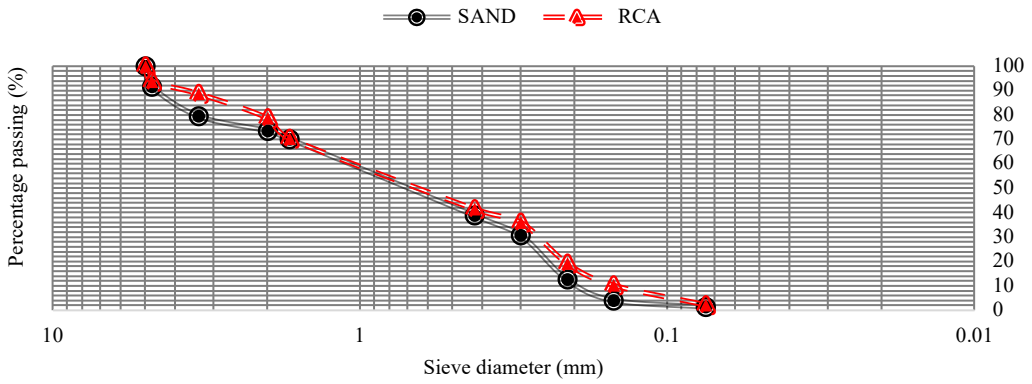

FIGURE 3. Particles size distribution of sand and RCA comparison curve

(a) (b)

FIGURE 4. The size particle distribution: (a) the sand distribution; (b) the RCA distribution

.

The cube mould seen in Figure 5(b) was used to create cubes measuring 50 mm × 50 mm × 50 mm. These cubes were used to measure the compressive strength of mortar containing 50% RCA. The cubes' compressive strength was assessed at 7, 14, and 28 days of age. As indicated by the schematic picture, 360 mm in length, 100 mm in breadth, and 100 mm in thickness (Nor et al. 2023) were used to create the interlocking concrete blocks. It is acceptable to utilise the block as a partition. The block's tongue and groove are included in the length. The tongue and groove measured 15 mm in length. Two varieties of interlocking concrete blocks were created, as depicted in Figure 6, respectively: a solid and THICB. The mortar's dry phase following casting. After the sample dries, the pipe will become stuck and be difficult to remove, so the PVC needs to be removed within five to fifteen minutes of casting as illustrated in Figure 7.

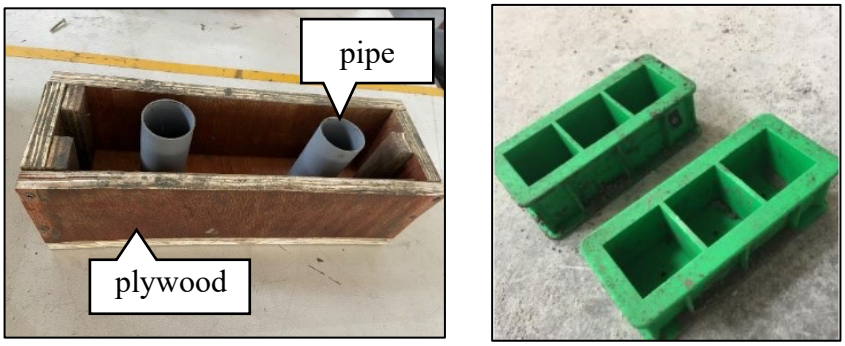

(a) (b)

FIGURE 5. The formwork: (a) THICB (b) cube 50 mm x 50 mm x 50 mm mould

(a)

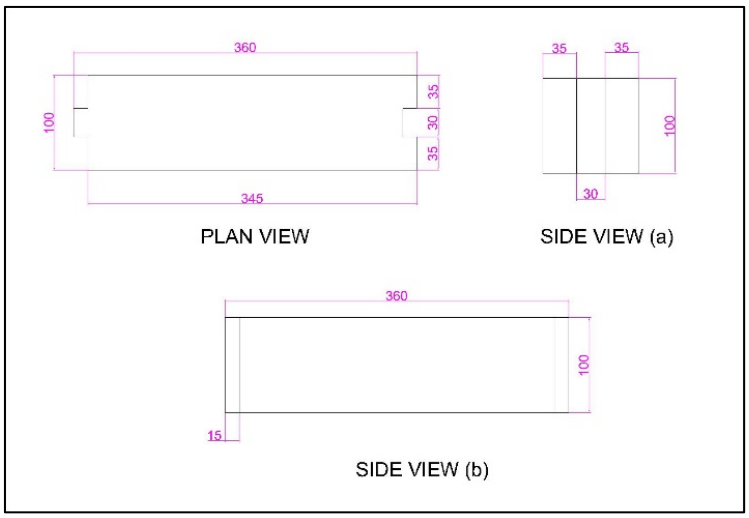

(b)

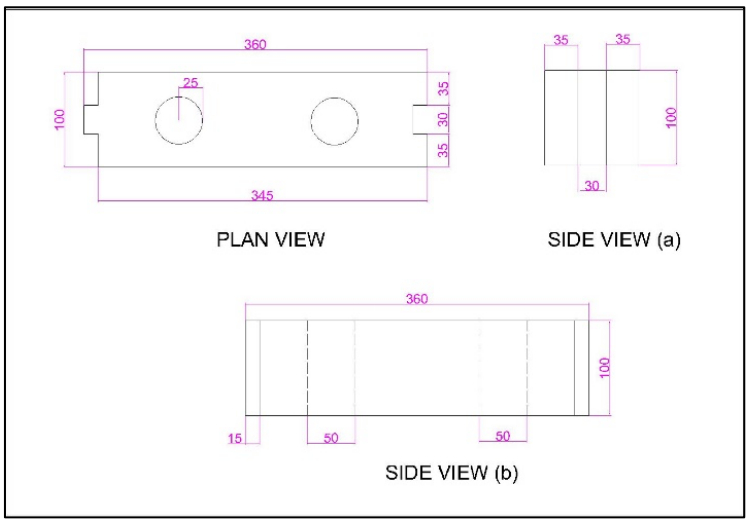

FIGURE 6. The schematic diagram of: (a) SICB (b) THICB (unit in mm)

FIGURE 7. The mortar in dry process

TESTING OF THE FRESH MORTAR

The purpose of the flowability test was to determine whether the newly mixed mortar containing RCA was suitable for use in a variety of construction applications. During the process, a typical device, such as a flow table, was used to hold a representative sample of the substance. A circular, flat plate that could be raised and let to fall freely made up the flow table. After positioning the sample in the middle of the table, the plate was repeatedly raised and lowered. The material spread outwards as a result of the falling plate's collision and its own weight during this process. Figure 8 depicts the flow-table test using the flow table tray, the mould, and the tiny rod.

The flowability of the mortar containing RCA was determined by how much the material spread and the nature of the ensuing flow pattern. Better flowability was indicated by a more fluid and spreading pattern, whereas lower flowability was indicated by a stiffer or less spread pattern. The test's outcomes were crucial in confirming that the material satisfied the particular needs of the intended use and could be easily laid, compacted, and moulded during construction.

FIGURE 8. The flow-table set testing

COMPRESSIVE STRENGTH TEST

A compression test can be used to evaluate how mortar containing RCA behaves under compressive load. The test specimen was clamped between two plates in order to conduct compression testing. The test specimen was then subjected to a force by means of bringing the crossbars together. 50 mm x 50 mm x 50 mm concrete cubes were utilised. For seven, fourteen, and twenty-eight days, the printing machine gathers three cube samples on average. Subsequently, the concrete cube was crushed until it broke against the steel plate.

FLEXURAL STRENGTH TEST

THICB measuring 360 mm x 100 mm x 100 mm were subjected to a flexural strength test in comparison to SICB that had been cured in water for 7, 14, and 28 days. A 100 kN universal testing equipment was used to conduct the test in accordance with BS EN 13523-7:2001. Both LVDT and strain gauge tests were used to get the deflection test results. The concrete blocks' flexural strength was evaluated using the three-point loading method (Chachar et al. 2022; Chen et al. 2022; Nor et al. 2023; Velay-Liazancos et al. 2018; Zhao et al. 2019). The span between supports was fixed at 270 mm, and the load was applied in the centre of each block. The average values for the maximum force and maximum stress were found using three specimens. The maximum force and stress values of SICB were compared in this study.

Once the interlocking block was placed on the measuring platform, the acquisition system and power supply were connected for the initial readings. The strain gauge utilised in the study was a Kyowa gauge model, shown in Figure 9(a). The testing apparatus was calibrated and running at a steady displacement rate of 0.2 mm/min in displacement control mode. As seen in Figure 9(b), strain gauges, which measure force or strain, were set up to the specimen at 180 mm in the centre of interlocking blocks, while linear variable deflection transformers (LVDT) were attached to monitor the deflection.

One strain gauge was installed and the concrete strain development at different depths was measured using 100 mm lengths. The installation of the strain gauge and LVDT with the universal testing machine is shown in Figure 10. Two supports and one LVDT were positioned at the pure bending region to monitor the growth of the mid-span deflection. A static data logger was used to record the strain and deflection data.

.

(a) (b)

FIGURE 9. The installation of the strain gauge: (a) strain gauge; (b) after installed

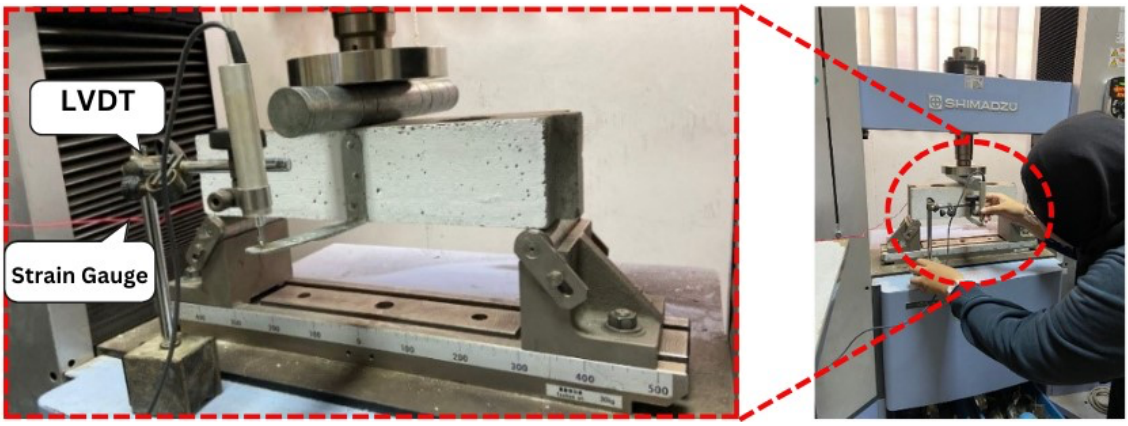

(a) (b)

FIGURE 10. The Installation of Strain Gauge and LVDT with the Universal Testing Machine (UTM): (a) the enlargement; (b) test set-up

RESULTS AND DISCUSSION

COMPRESSIVE STRENGTH

Using 50 mm x 50 mm x 50 mm cubes, the compressive strength was measured after 7, 14, and 28 days of cure. Nine samples for each of the three distinct batch combinations and each curing period made up the total of 27 samples that were manufactured. Since different people may have different findings, multiple samples were analysed to verify accuracy. A more accurate picture of the overall performance can be obtained by averaging the outcomes of several samples (Ghoniem et al. 2022; Tam et al. 2018). Based on the Table 3 and Figure 11, the average of the compressive strength of each curing age. The average values of the three distinct batch samples at varying curing ages. In result, after 7 days of curing, the compressive strength of the first batch was 27.8 kN, the second batch was 33.83 kN, and the last batch was 27.54 kN. The average compressive strength at 7 days was 29.72 kN. There were a few minor data inconsistencies that could be attributed to different testing conditions. In comparison to the preceding batches, Batch 2 showed somewhat higher values. All of the data, meanwhile, fell within a respectable range around the mean compressive strength. An illustration of the observed cracking patterns in the 7 days samples from batch 1 is shown in Figure 12 (a).

Additionally, 14 days after curing, the compressive strength tests were carried out. The first batch showed a compression of 27.32 kN, the second batch showed 33.04 kN, and the last batch showed 38.09 kN. The average compressive strength at 14 days was 32.82 kN. The results point to a gradual increase in compressive strength, with small variations that might be influenced by the circumstances of the test. However, there were no notable departures from the mean compressive strength; instead, the values fell within an acceptable range. It is necessary to test three samples or more

per batch in order to compute an average value and account for any variances.

Furthermore, data on compressive strength was gathered 28 days following cure. The compression values for the first, second, and last batches were 32.82 kN, 37.59 kN, and 33.67 kN, respectively. As in the earlier instances, minute changes in the test environment, like the weather, might have had an impact on the data collected. Consequently, the sample's average strength of 86.73 MPa and average force of 34.69 kN were recorded 28 days after curing, when the highest force in kN was detected. Figure 12 illustrates that the mix's initial compressive strength was higher than anticipated due to the use recycled concrete cubes in place of fine particles. A higher ratio of RCA can have negative impacts on concrete, according to research by Rezaei et al. (2023) that looked into the usage of recycled concrete aggregate in concrete. Age of curing boosts strength. As a result, the curve increased steadily since the curing age, which was 28 days, was the highest value. The damage to the cube samples from the compression test is depicted in Figures 12(b) and 12(c), which demonstrate the crack pattern at 14 and 28 days, respectively. The 28 days fractures were marginally offset from the cube sample, however the 7, and, 14 days cracks were clearly evident throughout.

TABLE 3. The average compressive strength of cubes by sample age

Sample Age (Day)	Load (kN)	Compressive Strength (MPa)
7	29.72	74.31
14	32.82	82.03
28	34.69	86.73

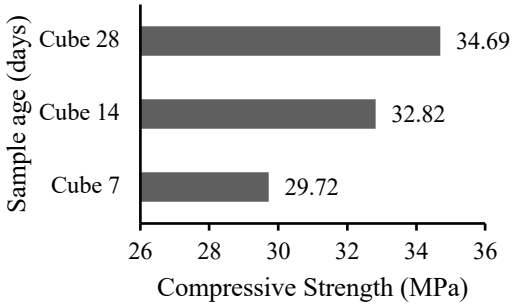

FIGURE 11. Average compressive strength of 7, 14, and 28 days of curing in MPa.

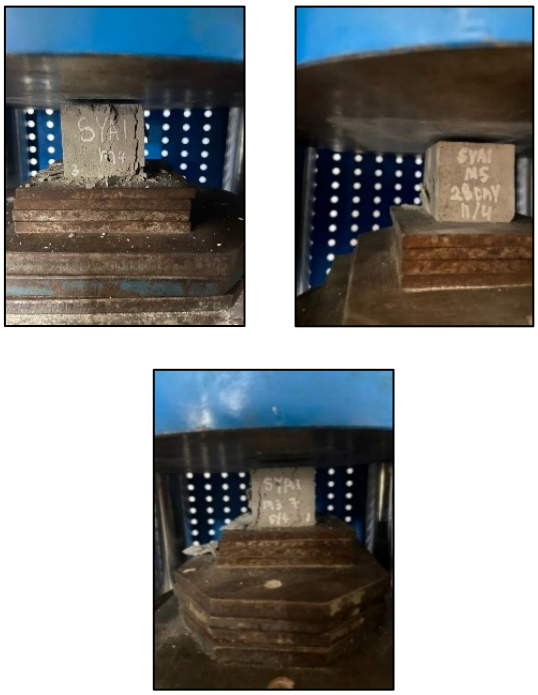

FIGURE 12. The crack pattern of cubes: (a) 7 days samples; (b) 14 days samples; (c) 28 days

FLEXURAL STRENGTH OF THE INTERLOCKING CONCRETE BLOCKS

THICB measuring 360 mm x 100 mm x 100 mm underwent a flexural strength test in comparison to SICB that had undergone 7, 14, and 28 days of water curing. According to BS EN 13523-7:2001, the test was conducted with a Universal Testing Machine 100 kN. Additionally, the findings of the deflection test came from the LVDT and strain gauge tests.

The three-point loading technique was employed to gauge the concrete blocks' flexural strength. The load was applied in the centre of each concrete block, and the span between the supports was set at 270 mm. Three specimens were used to get the maximum force and maximum stress average values. In this study, SICB values for maximum force and stress were compared.

The THICB sample features two 50 mm surface hollows, with deformation monitored using LVDTs. As shown in Table 4, the average maximum force recorded was 6437.26 N. Correspondingly, the THICB achieved an average flexural strength of 3.186 N/mm² at 7 days. These results indicate that the flexural performance of the samples exhibits a promising initial response.

The flexural strength of THICB was assessed for samples aged 14 days, with three samples collected to determine the average data. Compared to the 7 days data, the average maximum force for

the 14 days samples is 9353.01 N, indicating an increase. Furthermore, there was a rise in average maximum strength of 3.788 N/mm^2. As such, the 14 days samples' flexural strength behaviour is consistent with the 7 days samples' behaviour. In a similar procedure, flexural strength testing was done on THICB samples for 28 days curing age. The average data for these samples was represented by three samples. The 28 days samples had an average maximum force of 14058.63 N, which is higher than the 7 days samples. Furthermore, there is a 6.062 N/mm^2 increase in the average maximum strength. Consequently, the flexural strength behaviour observed in the 28 days samples, along with those aged 7 days, indicates the correct progression of strength over the curing period.

Table 5 and Figure 13 present the flexural strength of SICB at 7, 14, and 28 days. The average flexural strength recorded at each interval was 6148.67 N, 7600.81 N, and 14,455.23 N, respectively, indicating a progressive increase over time. Table 6 presents a comparison of the flexural strength between SICB and THICB, both of which utilize a 50% replacement of fine aggregates with recycled concrete aggregates. The primary design distinction is in the block configuration: THICB incorporates surface hollows, while SICB remains fully solid. As illustrated in Figure 14, both block types demonstrate an increasing trend in flexural strength over time, with only slight variations in their ultimate load capacities. Figure 15 further highlights the progressive development of flexural strength at 7, 14, and 28 days, with THICB consistently achieving higher strength values than SICB. At 14 days, the strength difference between THICB and SICB was merely 0.9829 N/mm², indicating minimal variation in performance at this stage.

As shown in Table 5, the flexural strength of SICB increases over time, similar to that of THICB. However, their structural designs differ significantly—THICB features two surface hollows measuring 50 mm each, whereas SICB is fully solid with no voids. These design differences form the basis for comparing their flexural strength performance.

TABLE 4. Flexural strength of two-hollow interlocking concrete block

Sample age (day)	Batch name	Ultimate load (N)	Average force	Stress (N/mm^2)	Average stress
7	1	5345.90	6437.26	2.64622	3.186
	2	7641.03		3.78231	
	3	6324.85		3.13080	
14	1	6377.32	9353.01	2.58281	3.788
	2	12211.9		4.94582	
	3	9469.80		3.83527	
28	1	12259.7	14058.63	6.06855	6.062
	2	15424.1		6.24718	
	3	14491.1		5.86890	

TABLE 5. Flexural strength of solid interlocking concrete block

Sample age (day)	Batch name	Ultimate load (N)	Average force	Stress (N/mm^2)	Average stress
7	1	6029.88	6148.67	2.225	2.268
	2	6140.77		2.265	
	3	6275.35		2.315	
14	1	6161.36	7600.81	2.273	2.804
	2	5662.97		2.089	
	3	10978.10		4.050	
28	1	14572.4	14455.23	5.377	5.333
	2	15060.5		5.067	
	3	13732.8		5.557	

At the 7 days curing age, THICB exhibited a slightly higher flexural strength than SICB, with a difference of only 288.59 N. This early performance suggests that THICB benefited from effective curing and initial material strength. By 14 days, the strength of THICB continued to rise, surpassing SICB by 1752.2 N, further confirming its early-age advantage. Overall, THICB outperformed SICB at both 7 and 14 days. However, at 28 days, the trend reversed slightly, THICB recorded a marginally lower maximum force of 14,058.63 N compared to SICB, which reached its peak at 14,455.23 N.

The flexural strength of both THICB and SICB increases linearly over the curing periods of 7, 14, and 28 days, based on their average maximum strength values. The plotted curves show a consistent upward trend for both types, with closely aligned trajectories. THICB achieved the highest strength of 6.0615 N/mm² at 28 days, followed by 3.7879 N/mm² at 14 days and 3.1864 N/mm² at 7 days. Notably, the 7-day strength of THICB exceeded SICB by approximately 2.268 N/mm². At 14 days, the difference between THICB and SICB narrowed to 0.9829 N/mm², indicating only a slight variation. At 28 days, SICB reached 5.333 N/mm², which was 0.7285 N/mm² lower than THICB.

These findings suggest that the solid configuration of SICB offers superior strength compared to the two-hollow design of THICB. The presence of central voids in THICB reduces its ultimate load capacity and overall stiffness, making it more prone to bending under applied loads. Cracking consistently occurred at the center of the hollow block, where tensile stress concentration was highest during bending—consistent with findings reported by Mohammed et al. (2018)..

TABLE 6. The comparison of average strength of the interlocking concrete block containing 50% of RCA.

Performance	Interlocking concrete block	Age of specimens (days)		
		7	14	28
Ultimate load (N)	Solid	6148.67	7600.81	14455.23
	Two-hollow	6437.26	9353.01	14058.63
	% difference	4.48	18.73	2.82
Flexural strength (N/mm^2)	Solid	2.268	2.804	5.333
	Two-hollow	3.186	3.788	6.062
	% difference	28.81	25.98	12.03

Figure 15 illustrates the strain–deflection relationship of the THICB at 7, 14, and 28 days of curing. In this study, the recorded maximum strain values showed inconsistency across the curing ages, likely influenced by the block's geometry. As highlighted by Nor et al. (2023), the voids within ICBs create additional space for expansion under load, affecting the strain distribution. Moreover, the non-uniform material distribution due to these voids can further influence the overall strain behavior. Indeed, elongation refers to the stretching or deformation of the interlocking block under applied loads, similar to deflection. Strain in a material is influenced by several factors, including its material properties, geometry, and loading conditions (Nor et al., 2023).

Despite these variations, THICB demonstrated favorable strength characteristics, supporting the viability of inclusion RCA into mortar mixtures for structural applications. These findings indicate the potential for commercializing THICB as a sustainable construction solution. Although RCA reduces overall strength compared to natural aggregates, its integration in innovative designs such as interlocking concrete blocks can still offer practical advantages, aligning with the industry's ongoing pursuit of performance-enhancing and environmentally responsible construction technologies.

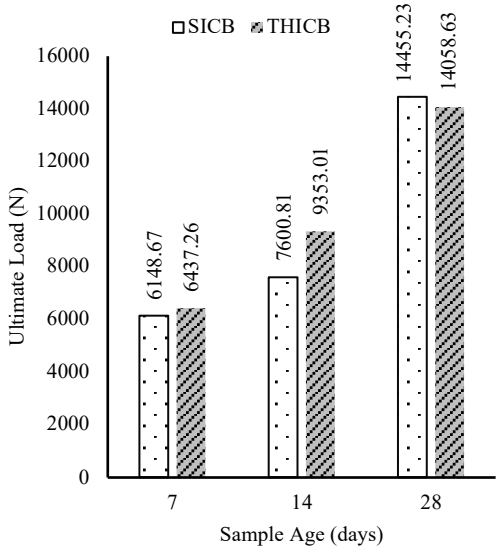

FIGURE 13. Ultimate load of SICB and THICB at different curing ages.

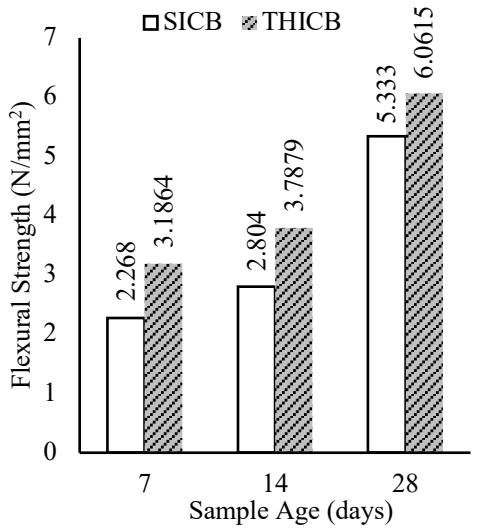

FIGURE 14. Average flexural strength of SICB and THICB at 7, 14 and 28 days.

CRACK PATTERN OF TWO-HOLLOW INTERLOCKING CONCRETE BLOCKS

Figure 16 illustrates the crack patterns observed in THICB at 7, 14, and 28 days of curing. When analyzing concrete cracking, it is sometimes possible to identify a single primary cause; however, in many cases, the pattern results from multiple contributing factors. Crack formation in reinforced concrete elements can be complex, involving interactions between geometry, loading type, support conditions, and the bond between concrete and reinforcement. These factors collectively influence crack development and, to some extent, can be understood, controlled, or optimized (Rasmussen et al., 2017). Flexural cracks typically occur at locations where bending moment stresses are greatest (Chiu et al., 2018).

The crack pattern in the THICB under maximum applied load was analyzed through visual inspection. It was observed that vertical fissures developed in the block following the application of a central point load. These vertical cracks are often indicative of structural failure in concrete elements. As shown in Figure 16 (a), THICB samples at 7 days exhibited the most prominent crack, measuring approximately 80 mm in length. In comparison, Figure 16 (b) displays the crack development after 14 days of curing, where the crack length reduced to 58 mm. By 28 days, as illustrated in Figure 16 (c), the crack length further decreased to 25 mm, indicating improved structural integrity with increased curing age.

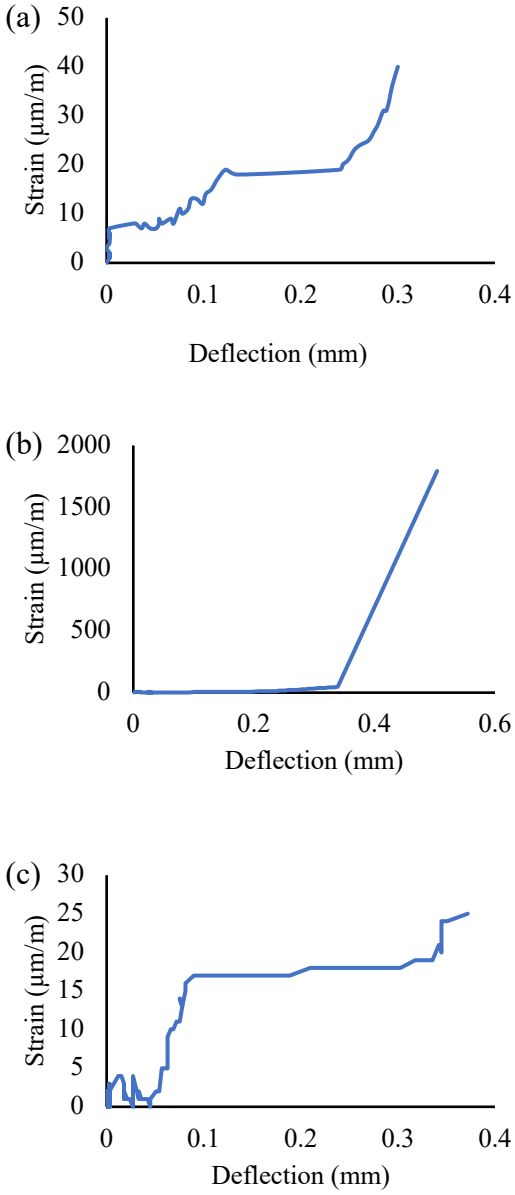

FIGURE 15. Strain-deflection relationships of THICBs at (a) 7 days; (b) 14 days; (c) 28 days

The cracks typically appeared at mid-height along the vertical axis of the THICB, indicating flexural failure initiated in the tensile zone, from the soffit of the block. Flexural cracks generally begin as fine surface fissures in tension zones and may remain small initially. However, under sustained loading, these cracks can widen and propagate uniformly across the member. This behaviour aligns with typical flexural stress responses in interlocking block systems. Table 7 provides a detailed summary of the observed cracking patterns across the different curing ages.

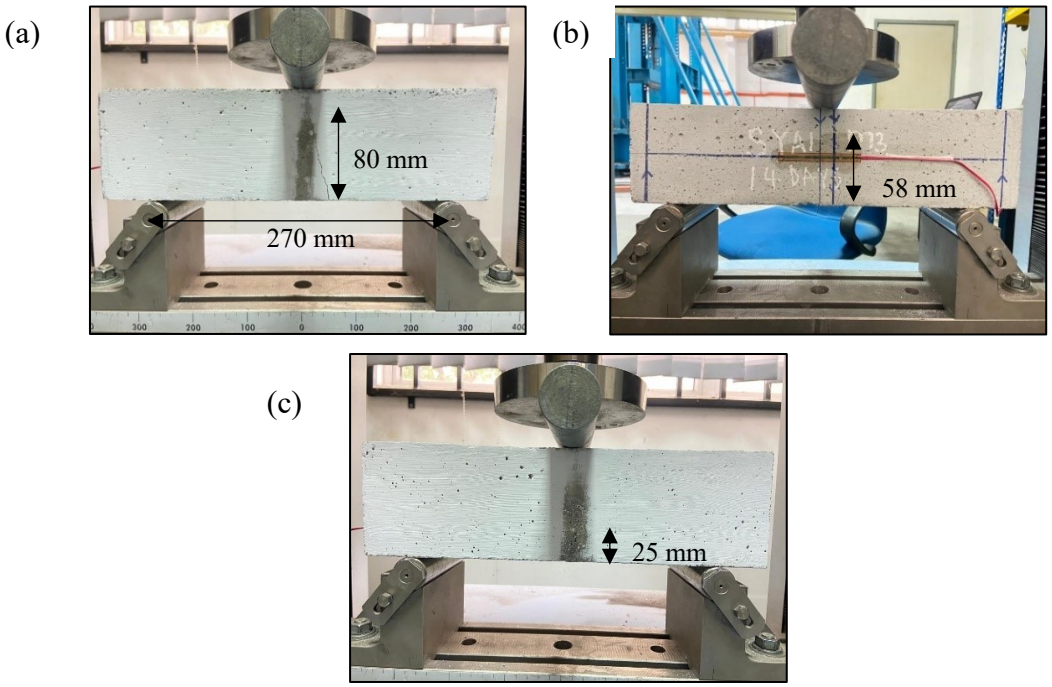

FIGURE 16. The crack growth of THICB of; (a) 7 days, (b) 14 days, (c) 28 days.

TABLE 7. Information on flexural crack of ICB

Member	Crack type	Important characteristics	Possible reason
Interlocking concrete block	Flexural crack interlocking concrete block	Originates in the region of maximal moment May be single or multiple cracks Maximum width at bottom/top of block	The specimen's flexural capacity is not sufficient. Due to heavy load, and the tension of the block occurs Due to maximum bending moment inside the block, and insufficient concrete cover

(Source: De Thales et al., 2022)

WATER ABSORPTION

The water absorption test involves measuring the weight of THICB samples in a saturated condition after curing periods of 7, 14, and 28 days, followed by oven-drying for 24 hours and calculating the percentage of water absorbed. In accordance with ASTM C140, nine THICB specimens containing RCA were tested. The average water absorption recorded was 14.18% at 7 days, 9.82% at 14 days, and 3.58% at 28 days. These results indicate a decreasing trend in water absorption with increased curing age, signifying improved material density and durability. Notably, the 28-day absorption value falls within the acceptable range (4%–10%) for load-bearing blocks, suggesting the blocks meet standard criteria for structural use at a matured curing stage.

High water absorption in blocks can negatively impact mortar hydration during construction, as excessive moisture drawn from the mortar may weaken the bond between block and mortar. This reduction in bond strength can ultimately affect the structural integrity of masonry units (Abu Bakar et al., 2017). According to Prakash et al. (2023), water absorption is a reliable indicator of the quality and long-term performance of concrete materials.

Water Absorption

$$\text{Percentage (\%)} = \left(\frac{Ww - Wd}{Wd}\right) \times 100\% \qquad (1)$$

Where:
Ww = Weight of the material after saturation (in grams or kilograms)
Wd = Initial dry weight of the material (in grams or kilograms)

FLOWABILITY OF THE FRESH MORTAR

A flow test was conducted on freshly mixed mortar to assess its workability immediately after preparation. Three separate batches were tested, each incorporating a 50% replacement of fine aggregates with recycled concrete aggregate (RCA). To ensure accuracy and consistency, tests were performed on all three batches, and the final results were averaged. The flow table method, as outlined by Al-Fakih et al. (2018), was employed to evaluate the mortar's workability.

FIGURE 17. Workability assessment of fresh mortar: (a) condition immediately after placement in the mould; (b) after 15 drops of the flow table; (c) final spread showing flowability of the mortar.

Figure 17 (a) shows the initial condition after the mortar was placed into the mould and compacted with a tamping rod. At this stage, the mix appeared stable, with an appropriate moisture level. Figure 17 (b) illustrates the condition after 15 drops of the flow table, revealing visible spreading of the mortar, indicating an increasing loss of cohesion. Finally, Figure 17 (c) shows the result after 25 drops, where the mortar formed a uniform circular spread, suggesting good workability.

According to ASTM C143/C143M-17, the standard spread diameter for workable mortar varies by mix design but typically ranges up to 50 mm. In this study, the mortar mix achieved a consistent and acceptable spread, confirming its workability. The 1:2:2 mix proportion, comprising cement, sand, RCA, superplasticizer, and a controlled water content, produced a mortar with suitable consistency for application.

CONCLUSION

This study examined the mechanical properties and structural performance of ICBs incorporating 50% RCA as a partial replacement for fine aggregates. The findings demonstrated that compressive strength increased consistently with curing age, reaching a maximum of 34.69 MPa at 28 days, reflecting the material's continued development and maturity. Both solid and two-hollow block types showed improvements in flexural strength over time. While the solid block achieved a higher compressive load capacity (14.46 kN), the two-hollow block exhibited superior flexural performance, reaching 14.06 kN (6.062 N/mm²), attributed to its enhanced flexibility due to internal voids.

Water absorption tests confirmed that the two-hollow blocks met the required criteria for load-bearing applications, with a value of 3.58% at 28 days, ensuring effective bonding with mortar. The workability of the RCA-based mortar remained within acceptable limits, aided by superplasticizers that compensated for RCA's higher water absorption. Strain measurements further indicated that the geometry of hollow blocks contributed to lower maximum strain values, suggesting a more controlled deformation behavior under load.

Overall, the results confirm the viability of using RCA in the production of interlocking blocks, supporting sustainable construction initiatives. Future research should focus on enhancing the long-term durability of RCA-based mortars and improving RCA quality through effective treatment methods, thereby strengthening RCA's role in eco-efficient and resilient construction practices.

ACKNOWLEDGEMENT

The authors would like to thank the Ministry of Higher Education (FRGS/1/2022/TK0/UITM/02/16) and Universiti Teknologi MARA, Cawangan Pulau Pinang (600-RMC/FRGS 5/3 (045/2022)) for their research funding support.

DECLARATION OF COMPETING INTEREST

None.

REFERENCES

Awoyera, P. O., Olalusi, O. B., Ibia, S., & Arunachalam, K. P. (2021). Water absorption, strength and microscale properties of interlocking concrete blocks made with plastic fibre and ceramic aggregates. Case Studies in Construction Materials 15 e00677. https://doi.org/10.1016/j.cscm.2021.e00677

Al-Fakih, A., Mohammed, B. S., Nuruddin, F. B., & Nikbakht, E. (2018). development of interlocking masonry bricks and its' structural behaviour: a review. Paper IOP Conference Series: Earth and Environmental Science 140 012127. https://doi.org/10.1088/1755-1315/140/1/012127

Al-Fakih, A., Mohammed, B. S., Al-Shugaa, M.A., & Al-Osta, M.A. (2022). Experimental investigation of dry-bed joints in rubberized concrete interlocking masonry. Journal of Building Engineering 58 105048. https://doi.org/10.1016/j.jobe.2022.105048

Abu Bakar, B.H., Saari, S., & Surip, N.A. (2017). Water absorption characteristic of interlocking compressed earth brick units. AIP Conference Proceedings 1892, 020018. https://doi.org/10.1063/1.5005649

Abera, Y. & Shanko, A. 2022. Performance of concrete materials containing recycled aggregate from construction and demolition waste. Results in Materials 14: 100278. https://doi.org/https://doi.org/10.1016/j.rinma.2022.100278

Abro, F. U. R., Buller, A. S., Ali, T., Channa, I. A., Abdin, Z. U., & Zahee, S. A. (2024). Optimizing coal ash as a sustainable substitute of cement and aggregate in structural concrete. Jurnal Kejuruteraan 36(1) 2024: 191-198. https://doi.org/10.17576/jkukm-2024-36(1)-18

Bao, Z. 2023. Developing circularity of construction waste for a sustainable built environment in emerging economies: New insights from China. Developments in the Built Environment 13: 100107. https://doi.org/https://doi.org/10.1016/j.dibe.2022.100107

Chung, S. Y., Oh, S. E., Jo, S. S., Lehmann, C., Won, J., & Elrahman, M. A. (2023). Microstructural investigation of mortars incorporating cockle shell and waste fishing net. Case Studies in Construction Materials, 18. https://doi.org/10.1016/j.cscm.2022.e01719

Chandru, U., Bahurudeen, A., & Senthilkumar, R. (2023). Systematic comparison of different recycled fine aggregates from construction and demolition wastes in OPC concrete and PPC concrete. Journal of Building Engineering 75 106768. https://doi.org/10.1016/j.jobe.2023.106768

Chiu, C-K., Chi, K-N., & Ho, B-T. (2018). Experimental investigation on flexural crack control for high-strength reinforced-concrete beam members. International Journal of Concrete Structures and Materials. https://doi.org/10.1186/s40069-018-0253-8

Chen, Z. M., Kwong, K. Z., Lee, F. W. & Lim, J. H. (2022). Conceptual design of interlocking block utilizing lightweight expanded polystyrene concrete reinforced with kenaf fiber E3S. Web of Conferences 347 02014. https://doi.org/10.1051/e3sconf/202234702014.

Chachar, Z. A., Ali, I., Raza, M. S., Narwani, T. D., Raza, I., & Hussain, M. (2022). Flexural behavior of reinforced concrete beams by using rice husk ash as partial replacement of fine aggregates in cement concrete. Jurnal Kejuruteraan 34(4) 2022: 599-604. https://doi.org/10.17576/jkukm-2022-34(4)-08

Correia Lopes, G., Vicente, R., Azenha, M., & Ferreira, T. M. 2018. A systematic review of Prefabricated Enclosure Wall Panel Systems: Focus on technology driven for performance requirements. Sustainable Cities and Society 40: 688–703. https://doi.org/ https://doi.org/10.1016/j.scs.2017.12.027

De Thales, A.K.J., & KabirSadeghi. (2022). Causes and Effects of Structural Cracks. International Journal for Modern Trends in Science and Technology, 8(02): 64-69. https://doi.org/10.46501/IJMTST0802011

Ghoniem, A. (2022). Deep learning shear capacity prediction of fibrous recycled aggregate concrete beams strengthened by side carbon fiber-reinforced polymer sheets. Composite Structures 300 116137. https://doi.org/10.1016/j.compstruct.2022.116137

Hani, A. S., Norhayati, A. W., Ifaniza, I., & Ezdiani, M. M. (2024). Strength and water absorption properties of cement bricks containing sago fine waste. Jurnal Kejuruteraan 36(1) 2024: 62-70. https://doi.org/10.17576/jkukm-2024-36(1)-07

Klemun, M. M., Ojanperä, S., & Schweikert, A. 2022. Towards evaluating the effect of technology choices on linkages between

sustainable development goals. IScience, 105727. https://doi.org/https://doi.org/10.1016/j.isci.2022.105727

Li, L., Dabarera, A., & Dao, V. (2023). Assessment of cracking risk of concrete due to restrained strain based on zero-stress temperature and cracking temperature. Construction and Building Materials, 383. https://doi.org/10.1016/j.conbuildmat.2023.131381

Le, H-B., & Bui, Q-B. (2020). Recycled aggregate concretes – A state-of-the-art from the microstructure to the structural performance. Construction and Building Materials 257 119522. https://doi.org/10.1016/j.conbuildmat.2020.119522

Maysam, V.K., Siddaramaiah, Y.M., Jaideep, C. & Ganesh, A.C. (2022). An analytical studies on static and fatigue response of steel fibre and re-cycled aggregate integrated high strength concrete beam. Materials Today, 1 – 9. https://doi.org/10.1016/j.matpr.2022.05.282

Mohammed, B.S, Liew, M.S., Alaloul, W.S., Al-Fakih, A., Ibrahim, W., & Adamu, M. (2018). Development of rubberized geopolymer interlocking bricks. Case Studies in Construction Materials 8 (2018) 401–408. https://doi.org/10.1016/j.cscm.2018.03.007

Mohamed, N.A.G., Moustafa, A., & Darwish, E.A. (2024). Structural, acoustical, and thermal evaluation of an experimental house built with reinforced/hollow interlocking compressed stabilized earth brick-masonry. Journal of Building Engineering 86 108790. https://doi.org/10.1016/j.jobe.2024.108790

Nor, N. M., Setiawan, A. F., Fauzi, N. E. H. M., Zaini, M. N., Saliah, S. N. M., Nujid, M. M. & Ismail, S. A. (2023) The behaviour of one-hollow interlocking concrete block made from recycled concrete aggregate under flexural loading. Procedia Structural Integrity 47 732–43. https://doi.org/10.1016/j.prostr.2023.07.046

Nawaz, A., Chen, J., & Su, X. 2022. Factors in critical management practices for construction projects waste predictors to C&DW minimization and maximization. Journal of King Saud University - Science, 102512. https://doi.org/https://doi.org/10.1016/j.jksus.2022.102512

Rifa, A., Subhani, Sk. M., Bahurudeen, A., & Santhosh, K.G. (2023). A systematic comparison of performance of recycled concrete fine aggregates with other alternative fine aggregates: An approach to find a sustainable alternative to river sand. Journal of Building Engineering 78 107695. https://doi.org/10.1016/j.jobe.2023.107695

Rezaei, F., Memarzadeh, A., Davoodi, M.R., Dashab, M.A., & Nematzadeh, M. (2023). Mechanical features and durability of concrete incorporating recycled coarse aggregate and nano-silica: Experimental study, prediction, and optimization. Journal of Building Engineering 73 106715. https://doi.org/10.1016/j.jobe.2023.106715

Ruslan, A. K., Nor, N. M., Ramle, M. A., Jamaludin, A. H., Mat Saliah, S. N., Fauzi, M. A., Md Hassan, A. S., Tambichik, M. A., & Kasim, N. A. (2024). Mechanical behaviour slenderness ratio of 13 solid wall panels under uniformly distributed load. Jurnal Kejuruteraan 36(1) 2024: 09-19. https://doi.org/10.17576/jkukm-2024-36(1)-02

Patra, I., Al-Awsi, G. R. L., Hasan, Y. M., & Almotlaq, S. S. K. (2022). Mechanical properties of concrete containing recycled aggregate from construction waste. Sustainable Energy Technologies and Assessments 53 102722. https://doi.org/10.1016/j.seta.2022.102722

Prakash, O.S., Kuldeep, S.K., & Shailesh, C. (2023). strength studies on concrete containing of recycled coarse aggregate and granite cutting waste as partial replacement of fine aggregate. Materials Today: Proceedings, 76, 481–487. https://doi.org/10.1016/j.matpr.2022.11.153

Rasmussen, A.B., Fisker, J., Hagsten, L.G. (2017). Cracking in flexural reinforced concrete members. Procedia Engineering 172 (2017) 922 – 929. https://doi:10.1016/j.proeng.2017.02.102

Radonjanin, V., Malešev, M., Marinkovic, S., & Al Malty, A.E.S. (2013). Green recycled aggregate concrete. Construction and Building Materials 47 1503–1511. http://dx.doi.org/10.1016/j.conbuildmat.2013.06.076

Sanjay, K.V., & Manoj, K.T. (2022). Performance enhancement of the recycled aggregate concrete properties using blended sand. Materials Today, 1 – 6. https://doi.org/10.1016/j.matpr.2022.04.651

Shaikh, F. A., Bheel, N., Khoso, A. R. Raza, A., & Asadullah. (2022). Effect of crushed coconut shell and over burnt brick on the mechanical behaviour of green concrete as a partial replacement of coarse aggregate. Jurnal Kejuruteraan 34(6) 2022: 1027-1037. https://doi.org/10.17576/jkukm-2022-34(6)-04

Uygunog˘lu, T., Ilker, B.T., Osman, G., & Witold, B. (2012). the effect of fly ash content and types of aggregates on the properties of pre-fabricated concrete interlocking blocks (Pcibs). Construction and Building Materials 30 (2012), 180–187. http://doi:10.1016/j.conbuildmat.2011.12.020

Vázquez, E. (2016). Recycled aggregates for concrete: Problems and possible solutions. International Journal of Earth & Environmental Sciences 1:122. https://doi.org/10.15344/2456-351X/2016/122.

Velay-Lizancos, M., Vázquez-Burgo, P., Restrepo, D., & Martínez-Lage, I. (2018). Effect of fine and coarse recycled concrete aggregate on the mechanical behavior of precast reinforced beams: Comparison of FE simulations, theoretical, and experimental results on real scale beams. Construction and Building Materials 191 1109–19. https://doi.org/10.1016/j.conbuildmat.2018.10.075

Tam, V. W. Y., Soomro, M., & Evangelista, A. C. J. (2018). A review of recycled aggregate in concrete applications (2000–2017). Construction and Building Materials 172 272–92. https://doi.org/10.1016/j.conbuildmat.2018.03.240

Zhao, J., Li, G., Wang, Z., & Zhao, X. (2019). Fatigue behavior of concrete beams reinforced with glass- and carbon-fiber reinforced polymer (GFRP/CFRP) bars after exposure to elevated temperatures. Composite Structures 229 111427. https://doi.org/10.1016/j.compstruct.2019.111427

Zhang, C., Hu, M., Van der Meide, M., Di Maio, F., Yang, X., Gao, X., Li, K., Zhao, H., & Li, C. (2023). Life cycle assessment of material footprint in recycling: A case of concrete recycling. Waste Management 155 311–319. https://doi.org/https://doi.org/10.1016/j.wasman.2022.10.035

Zhu, L., Dai, J., Bai, G., & Zhang, F. (2015). Study on thermal properties of recycled aggregate concrete and recycled concrete blocks. Construction and Building Materials 94 620–628. http://dx.doi.org/10.1016/j.conbuildmat.2015.07.058